

Electronic Supplementary Information (ESI):

Self-assembled helical columnar superstructures with selective homochirality

Bin Mu, Qian Li, Xiao Li, Jian Chen, Jianglin Fang and Dongzhong Chen*

Table of contents

| | |
|--|-----|
| 1. Materials and measurements..... | S2 |
| 2. Thermal analysis..... | S3 |
| 3. Structural analysis..... | S6 |
| 3.1. SAXS/WAXS characterization and analysis for EDA complexes of <i>P</i> ₆ -100 doped with L-mTNF..... | S6 |
| 3.2. SAXS/WAXS characterization and analysis for EDA complexes of <i>P</i> ₉ -100 doped with L-mTNF..... | S17 |
| 3.3. SAXS/WAXS characterization and analysis for EDA complexes of monomers <i>P</i> _{<i>m</i>} -1 doped with L-mTNF..... | S24 |
| 4. CD and UV-vis spectroscopic measurements of EDA complexes in solution and in solid-state film..... | S25 |
| 5. Supplementary references..... | S30 |

1. Materials and measurements

Materials:

Two typical side-chain discotic LC polymers of six-methylene spacer P_6 -100 ($M_{n, GPC} = 16,000$ g mol⁻¹, PDI = 1.42) and nine-methylene spacer P_9 -100 ($M_{n, GPC} = 19,000$ g mol⁻¹, PDI = 1.37) with designed degree of polymerization DP = 100 were prepared through reversible addition fragmentation chain transfer (RAFT) polymerization according to similar procedures as reported previously.^{1,2} The preparation of electron acceptors of chiral ester derivatives of TNF was referred to the literature procedure.³ With 9-fluorenone-2-carboxylic acid (TCI, >96.0%) as the starting material, firstly a nitration process was carried out in the presence of fuming HNO₃ and concentrated H₂SO₄ to obtain the intermediate TNF-2-carboxylic acid, then after esterification reaction with L-(-)-menthol (TCI, >99.0%) or D-(+)-menthol (TCI, >99.0%), the chiral acceptor compounds denoted respectively as L-mTNF and D-mTNF were achieved.

The polymeric EDA complexes were prepared by co-dissolving of discotic LC polymers with predesigned amount of the chiral dopant L-mTNF or D-mTNF in dichloromethane, the mixtures were sonicated for 5 min and then removed the solvent through slow evaporation under stirring at room temperature, finally dried in a vacuum oven for 24 h to yield the doped EDA complexes in solid powder.

Measurements:

Differential scanning calorimetry (DSC) thermograms were recorded on a Perkin-Elmer Pyris I calorimeter equipped with a cooling accessory and under an argon atmosphere. Typically, about 5 mg of the solid sample was encapsulated in a sealed aluminum pan with an identical empty pan as the reference. Indium and zinc were used as the calibration standard. The polarized optical microscopy (POM) was adopted to investigate the phase transitions and photograph optical texture changes with a PM6000 microscope under crossed-polarizers equipped with a Leitz-350 heating stage and an associated Nikon (D3100) digital camera. X-ray scattering experiments were performed with a high-flux small-angle X-ray scattering instrument (SAXSess mc², Anton Paar) equipped with Kratky block-collimation system and a temperature control unit (Anton Paar TCS 120 and TCS 300). Both small angle X-ray scattering (SAXS) and wide angle X-ray scattering (WAXS) were

simultaneously recorded on an imaging-plate (IP) at 40 kV and 50 mA, with the q range covered by the IP was extended to high-angle range from 0.06 to 29 nm⁻¹, where $q = 4\pi\sin\theta/\lambda$, the wavelength λ is 0.1542 nm of Cu-K α radiation and 2θ is the scattering angle. The powder samples were encapsulated with aluminum foil during the measurement and the obtained X-ray analysis data were processed with the associated SAXSquant software 3.80 and the aluminum foil background signal was subtracted. Circular dichroism (CD) and Ultraviolet visible (UV) spectroscopy measurements were carried out in a Jasco J-810 Spectropolarimeter.

2. Thermal analysis

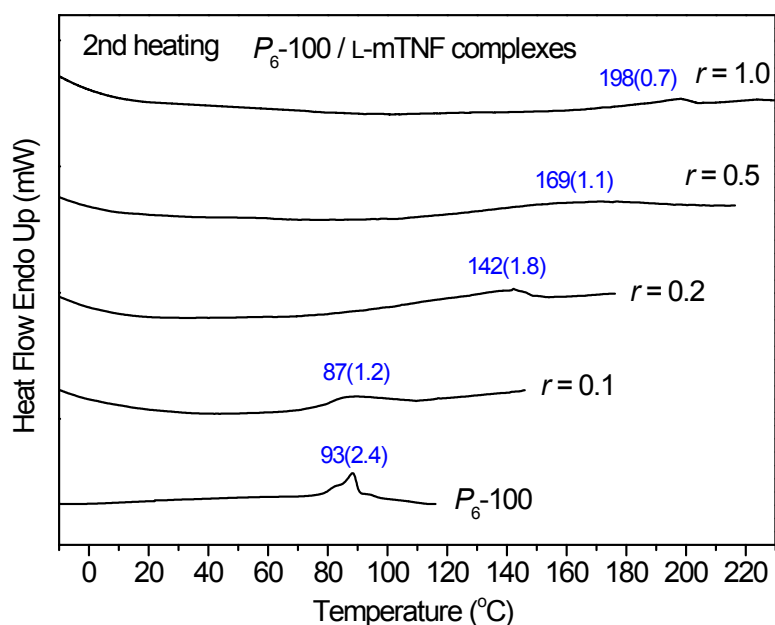


Figure S1. DSC traces of undoped P_6 -100 and its EDA complexes doped with L-mTNF in the second heating runs at a rate of 10 °C min⁻¹, where r represents the molar ratio of L-mTNF to triphenylene (TP) side-groups (mTNF/TP), the values in blue labeled on the curves denoting the transition peak temperatures and enthalpy changes [T / °C (J g⁻¹)], hereinafter the same.

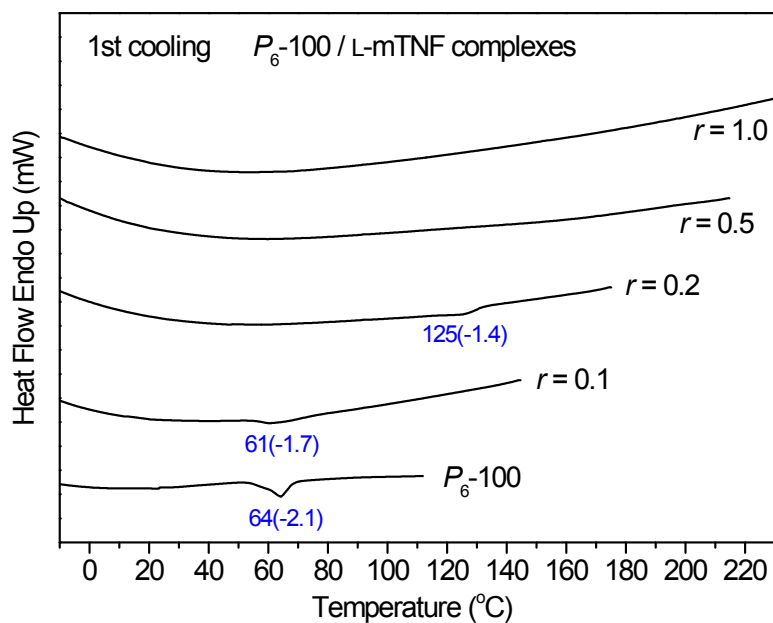


Figure S2. DSC traces of undoped P_6 -100 and its EDA complexes doped with L-mTNF in the cooling runs at a rate of $10\text{ }^\circ\text{C min}^{-1}$ [$T / ^\circ\text{C}$ (J g^{-1})].

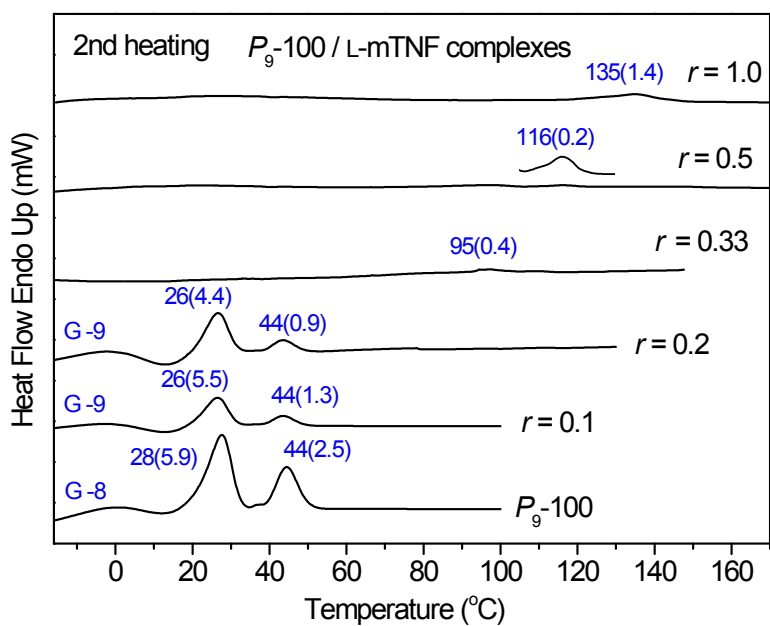


Figure S3. DSC traces of undoped P_9 -100 and its EDA complexes doped with L-mTNF in the second heating runs at a rate of $10\text{ }^\circ\text{C min}^{-1}$ [$T / ^\circ\text{C}$ (J g^{-1})].

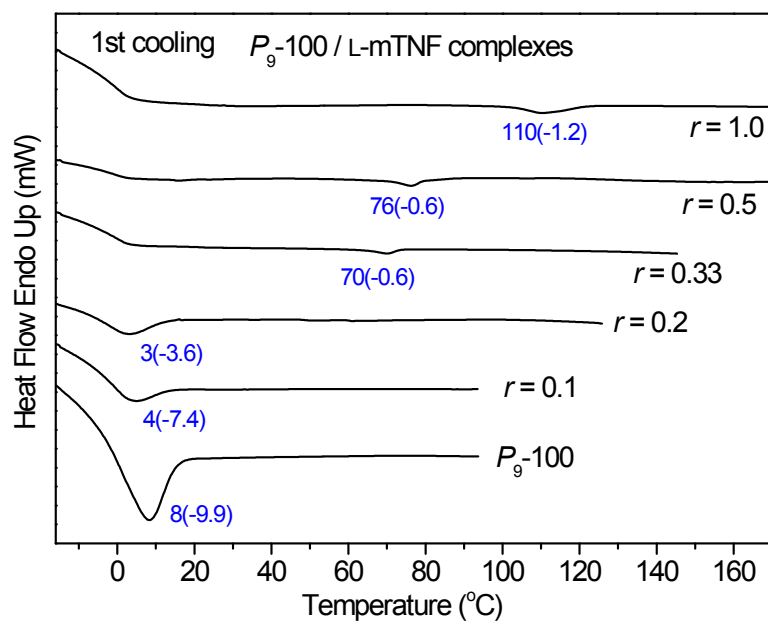


Figure S4. DSC traces of undoped P_9 -100 and its EDA complexes doped with L-mTNF in the cooling runs at a rate of $10\text{ }^\circ\text{C min}^{-1}$ [$T / ^\circ\text{C}$ (J g^{-1})].

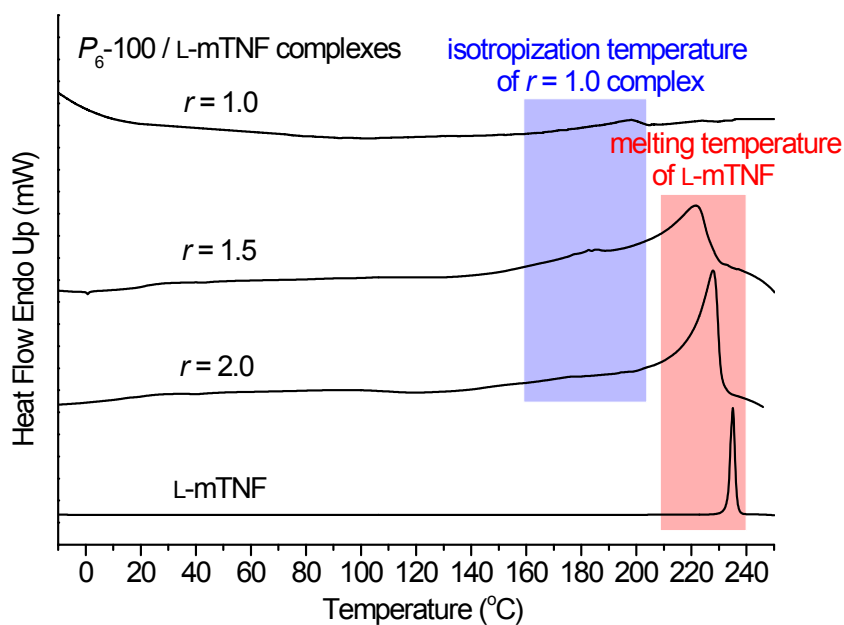


Figure S5. DSC traces of EDA complexes of P_6 -100 doped with L-mTNF in the molar ratio $r = \text{mTNF/TP}$ of 1.0, 1.5 and 2.0, and of the crystalline acceptor component L-mTNF in the first heating runs at a rate of $10\text{ }^\circ\text{C min}^{-1}$.

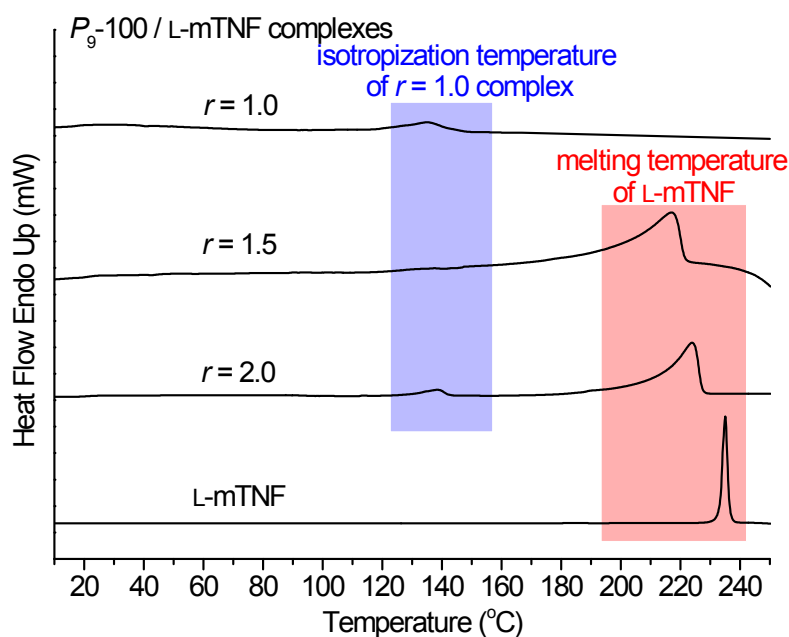


Figure S6. DSC traces of EDA complexes of P_9 -100 doped with L-mTNF in the molar ratio $r = \text{mTNF}/\text{TP}$ of 1.0, 1.5 and 2.0, and of the crystalline acceptor component L-mTNF in the first heating runs at a rate of $10\text{ }^\circ\text{C min}^{-1}$.

As shown in Figure S5 and S6, EDA complexes of TP-based side-chain discotic LC polymers P_m -100 (spacer methylene number $m = 6, 9$) doped with L-mTNF in the molar ratio r higher than 1.0 such as representative $r = 1.5$ and 2.0, exhibit two thermal transitions, of which one corresponds to isotropization transition temperatures of EDA complexes similar to that of $r = 1.0$ as highlighted by blue shadows, and the higher temperature transitions with much larger enthalpy changes are presumably associated with melting process of excessive acceptor component L-mTNF as indicated by pale red shadows. Therefore, it can be concluded that phase separation may occur when the molar ratio $r > 1.0$ with excessive electron acceptor component.

3. Structural analysis

3.1 SAXS/WAXS characterization and analysis for EDA complexes of P_6 -100 with L-mTNF

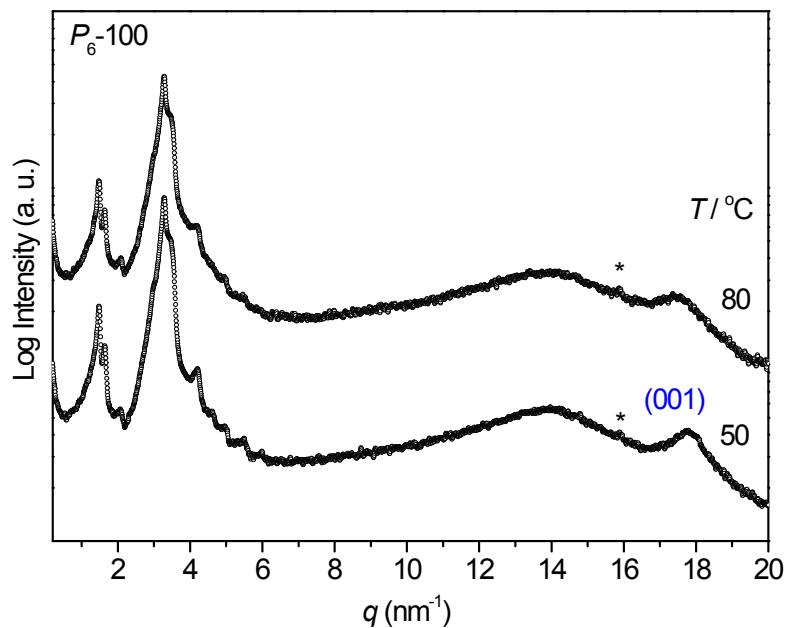


Figure S7. Variable-temperature SAXS/WAXS patterns of undoped P_6 -100 at indicated temperatures during the second heating process.

*The background peaks from the packing aluminum foil locating in the wide-angle region are labeled by asterisks, which have a negligible disturbance to the interested sample peaks thus without complete subtraction so as to avoid distortion of the peak shape and smoothing over some significant weak signals, hereinafter the same.

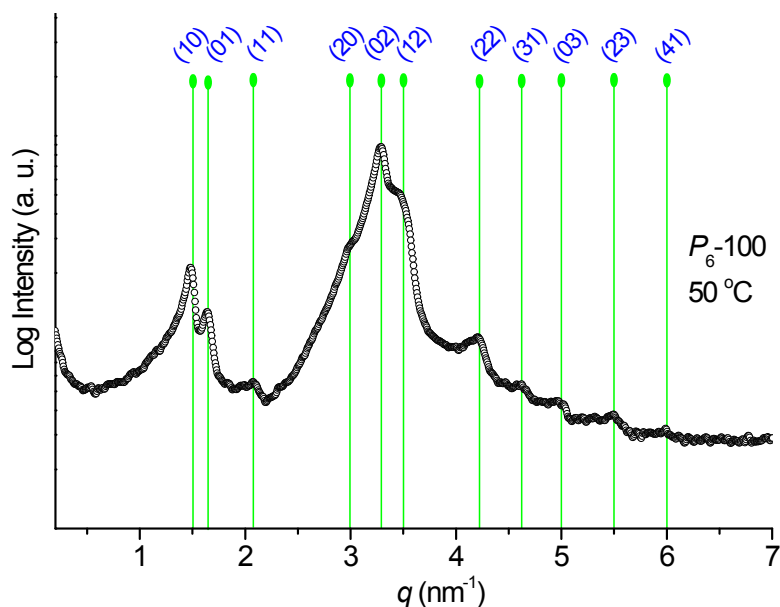


Figure S8. SAXS pattern with proposed indexing of undoped P_6 -100 at 50 °C during the second heating process.

The X-ray scattering signals assignment was referred to our previously published work,¹ and the SAXS/WAXS data for undoped P_6 -100 at 50 °C during the second heating process were summarized in the Table S1.

Table S1. SAXS/WAXS data for undoped P_6 -100 at 50 °C during the second heating process

| mesophase | hkl | d_{obs} [Å] | d_{cacl} [Å] | lattice parameter [Å] | ρ_{calc}^a | |
|--|-------|-------------------------|--------------------------|--------------------------|-------------------------|--|
| Col _{ob-s} (50 °C) $p2$ | 100 | 41.9 | 41.9 | $a = 42.1$ | 1.07 g cm ⁻³ | |
| | 010 | 37.9 | 37.9 | $b = 38.0$ | | |
| | 110 | 29.9 | 29.6 | $\gamma = 84.4^\circ$ | | |
| | 200 | 20.9 | 20.9 | | | |
| | 020 | 18.9 | 18.9 | | | |
| | 120 | 18.0 | 17.9 | | | |
| | 220 | 14.8 | 14.9 | | | |
| | 310 | 13.5 | 13.5 | | | |
| | 030 | 12.6 | 12.6 | | | |
| | 230 | 11.3 | 11.3 | | | |
| | 410 | 10.5 | 10.4 | | | |
| | | 4.5 (diffuse halo) | | | | |
| | | 001 | 3.52 | | | |

^a Density, ρ , was calculated as $\rho = M \cdot Z / (N_A \cdot V_{\text{unit cell}})$, where $V_{\text{unit cell}} = a \cdot b \cdot \sin \gamma \cdot c$, M is the molecular weight of the repeat unit of 899 g mol⁻¹, and $Z = 4$ ($c = 3.52$ Å).

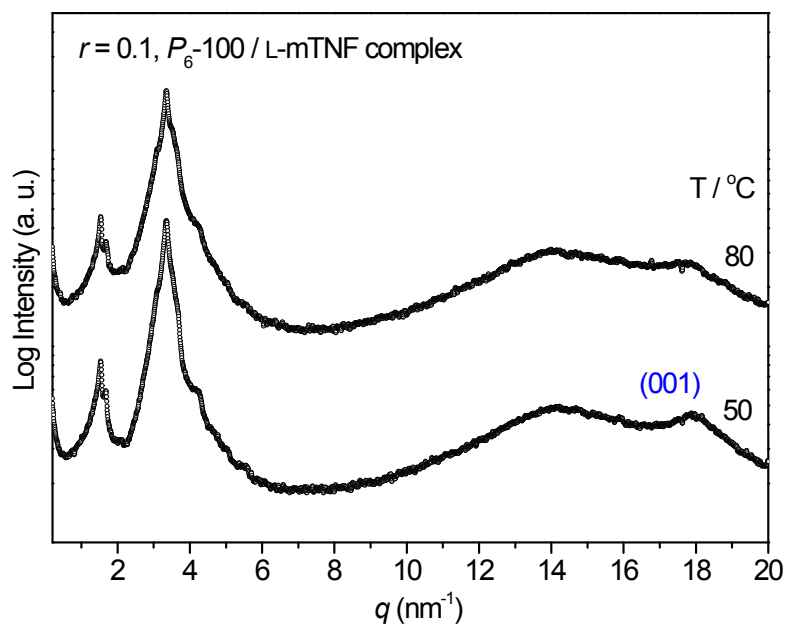


Figure S9. Variable-temperature SAXS/WAXS patterns of EDA complex of P_6 -100 doped with L-mTNF in the ratio $r = 0.1$ at indicated temperatures during the second heating process.

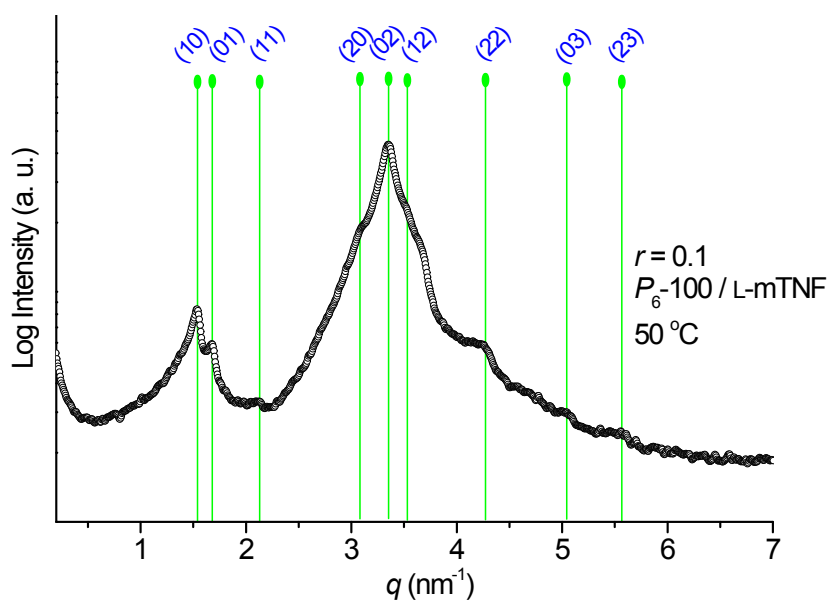


Figure S10. SAXS profile with proposed indexing of EDA complex of P_6 -100 doped with L-mTNF in the ratio $r = 0.1$ at 50 °C during the second heating process.

Table S2. SAXS/WAXS data for EDA complex of P_6 -100 doped with L-mTNF in the ratio $r = 0.1$ at 50 °C during the second heating process

| mesophase | hkl | d_{obs} [Å] | d_{cacl} [Å] | lattice parameter [Å] | ρ_{calc}^a |
|--|-------|-------------------------|--------------------------|--------------------------|-------------------------|
| Col _{ob-s} (50 °C) $p2$ | 100 | 41.1 | 41.1 | $a = 41.4$ | 1.05 g cm ⁻³ |
| | 010 | 37.4 | 37.4 | $b = 37.7$ | |
| | 110 | 29.5 | 29.5 | $\gamma = 83.0^\circ$ | |
| | 200 | 20.4 | 20.6 | | |
| | 020 | 18.8 | 18.7 | | |
| | 120 | 17.8 | 17.9 | | |
| | 220 | 14.7 | 14.8 | | |
| | 030 | 12.5 | 12.5 | | |
| | 230 | 11.3 | 11.3 | | |
| | | 4.4 (diffuse halo) | | | |
| | 001 | 3.51 | | | |

^a Density, ρ , was calculated as $\rho = M \cdot Z / (N_A \cdot V_{\text{unit cell}})$, where $V_{\text{unit cell}} = a \cdot b \cdot \sin \gamma \cdot c$, $Z = 4$ ($c = 3.51$ Å), and M is the average molecular weight of the repeat unit (899 g mol⁻¹) and doped L-mTNF (497 g mol⁻¹), which is calculated as $M = (899 + 497 \cdot r) / (1 + r) = 862$ g mol⁻¹.

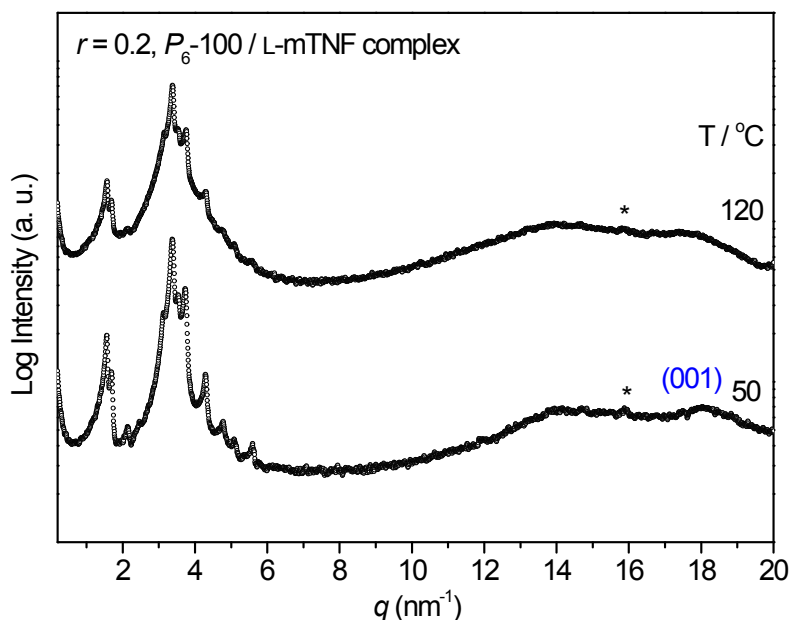


Figure S11. Variable-temperature SAXS/WAXS patterns of EDA complex of P_6 -100 doped with L-mTNF in the ratio $r = 0.2$ at indicated temperatures during the second heating process.

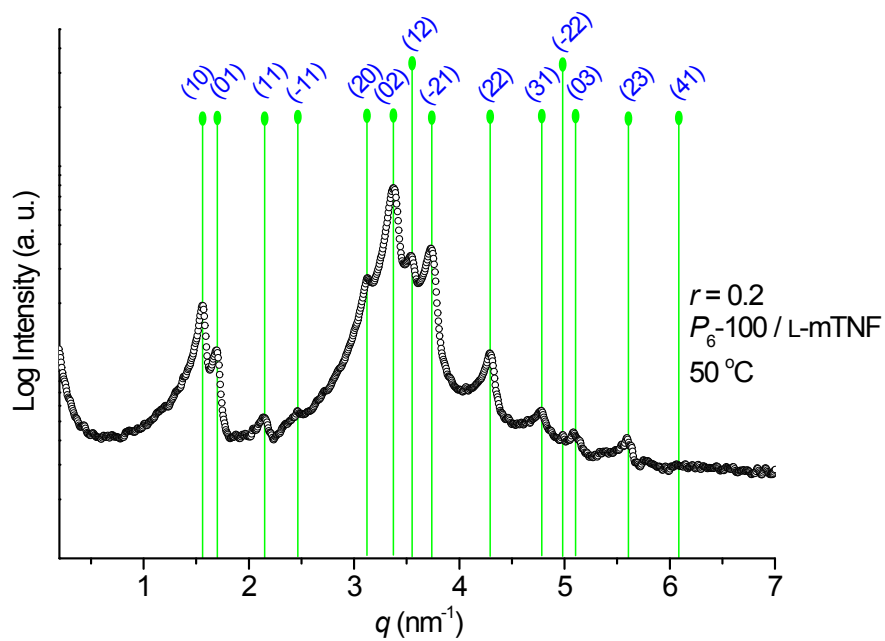


Figure S12. SAXS profile with proposed indexing of EDA complex of P_6-100 doped with L-mTNF in the ratio $r = 0.2$ at 50°C during the second heating process.

Table S3. SAXS/WAXS data for EDA complex of P_6 -100 doped with L-mTNF in the ratio $r = 0.2$ at 50 °C during the second heating process

| mesophase | hkl | d_{obs} [Å] | d_{cacl} [Å] | lattice parameter [Å] | ρ_{calc}^a |
|--|-------|-------------------------|--------------------------|--------------------------|-------------------------|
| Col _{ob-s} (50 °C) $p2$ | 100 | 40.3 | 40.3 | $a = 40.6$ | 1.06 g cm ⁻³ |
| | 010 | 37.0 | 37.0 | $b = 37.3$ | |
| | 110 | 29.2 | 29.2 | $\gamma = 82.6^\circ$ | |
| | -110 | 25.5 | 25.6 | | |
| | 200 | 20.1 | 20.2 | | |
| | 020 | 18.6 | 18.5 | | |
| | 120 | 17.7 | 17.7 | | |
| | -210 | 16.8 | 16.8 | | |
| | 220 | 14.6 | 14.6 | | |
| | 310 | 13.2 | 13.2 | | |
| | -220 | 12.6 | 12.8 | | |
| | 030 | 12.3 | 12.3 | | |
| | 230 | 11.2 | 11.2 | | |
| | 410 | 10.3 | 10.0 | | |
| | | 4.5 (diffuse halo) | | | |
| | 001 | 3.48 | | | |

^a Density, ρ , was calculated as $\rho = M \cdot Z / (N_A \cdot V_{\text{unit cell}})$, where $V_{\text{unit cell}} = a \cdot b \cdot \sin \gamma \cdot c$, $Z = 4$ ($c = 3.48$ Å), and M is the average molecular weight of the repeat unit (899 g mol⁻¹) and doped L-mTNF (497 g mol⁻¹), which is calculated as $M = (899 + 497 \cdot r) / (1 + r) = 832$ g mol⁻¹.

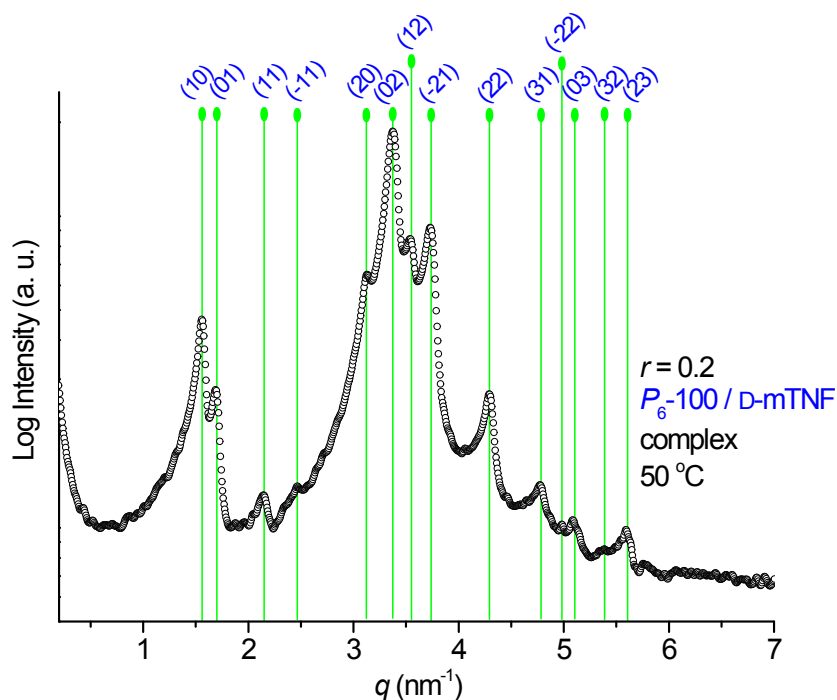


Figure S13. Representative SAXS pattern obtained from EDA complex of P_6 -100 doped with D-mTNF in the ratio $r = 0.2$ at $50\text{ }^\circ\text{C}$ during the second heating process.

As shown in Figure S13, the SAXS pattern obtained from representative sample of EDA complex of P_6 -100 doped with D-mTNF in the ratio $r = 0.2$ exhibited nearly the same as that of corresponding polymer complex with enantiomeric L-mTNF (Figure S12), demonstrating the definite self-assembled structures determined only by the mTNF/TP molar ratio irrespective of enantiomeric nature of the doped acceptor components, while the enantiomeric nature of the triggered dopant specified the discriminating homochirality of the polymeric EDA complexes.

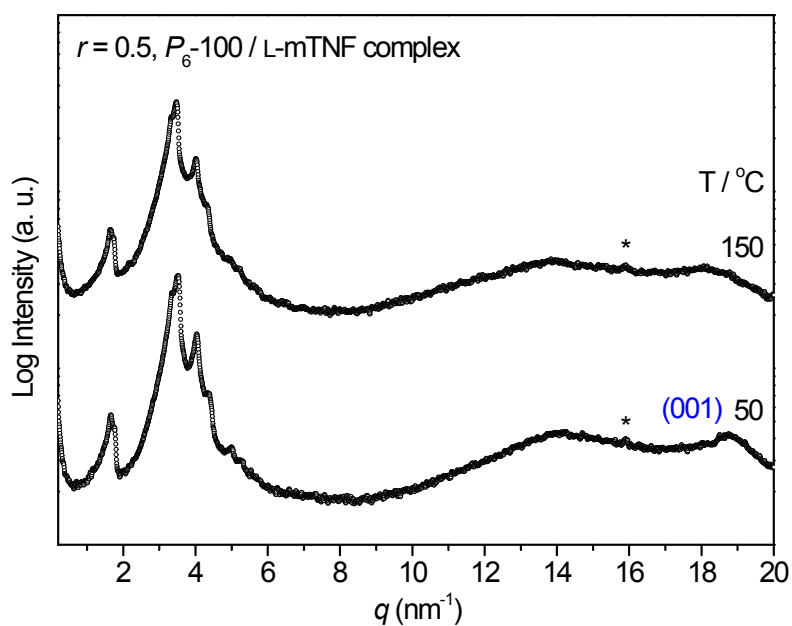


Figure S14. Variable-temperature SAXS/WAXS patterns of EDA complex of P_6 -100 doped with L-mTNF in the ratio $r = 0.5$ at indicated temperatures during the second heating process.

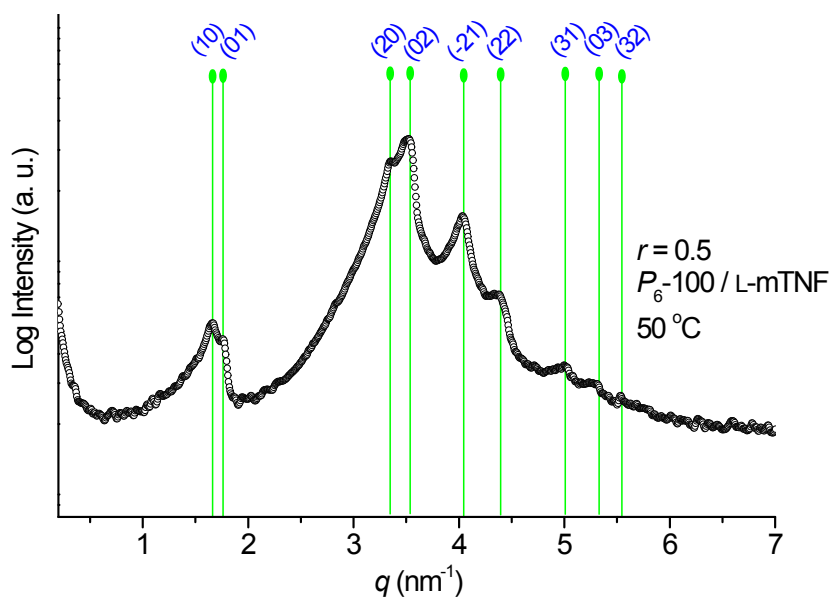


Figure S15. SAXS profile with proposed indexing of EDA complex of P_6 -100 doped with L-mTNF in the ratio $r = 0.5$ at 50 °C during the second heating process.

Table S4. SAXS/WAXS data for EDA complex of P_6 -100 doped with L-mTNF in the ratio $r = 0.5$ at 50 °C during the second heating process

| mesophase | hkl | d_{obs} [Å] | d_{cacl} [Å] | lattice parameter [Å] | ρ_{calc}^a |
|--|-------|-------------------------|--------------------------|--------------------------|-------------------------|
| Col _{obs} -s (50 °C) $p2$ | 100 | 37.6 | 37.6 | $a = 38.3$ | 1.11 g cm ⁻³ |
| | 010 | 35.3 | 35.5 | $b = 36.1$ | |
| | 200 | 18.8 | 18.8 | $\gamma = 79.3^\circ$ | |
| | 020 | 17.8 | 17.8 | | |
| | -210 | 15.6 | 15.5 | | |
| | 220 | 14.3 | 14.3 | | |
| | 310 | 12.6 | 12.6 | | |
| | 030 | 11.8 | 11.8 | | |
| | 320 | 11.4 | 11.3 | | |
| | | 4.5 (diffuse halo) | | | |
| | 001 | 3.36 | | | |

^a Density, ρ , was calculated as $\rho = M \cdot Z / (N_A \cdot V_{\text{unit cell}})$, where $V_{\text{unit cell}} = a \cdot b \cdot \sin \gamma \cdot c$, $Z = 4$ ($c = 3.36$ Å), and M is the average molecular weight of the repeat unit (899 g mol⁻¹) and doped L-mTNF (497 g mol⁻¹), which is calculated as $M = (899 + 497 \cdot r) / (1 + r) = 765$ g mol⁻¹.

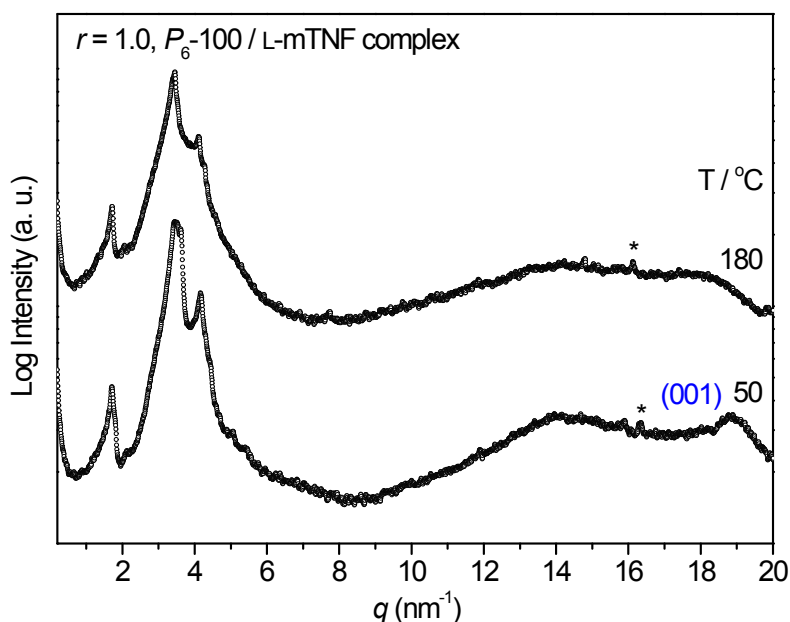


Figure S16. Variable-temperature SAXS/WAXS patterns of equimolar EDA complex of P_6 -100 doped with L-mTNF ($r = 1.0$) at indicated temperatures during the second heating process.

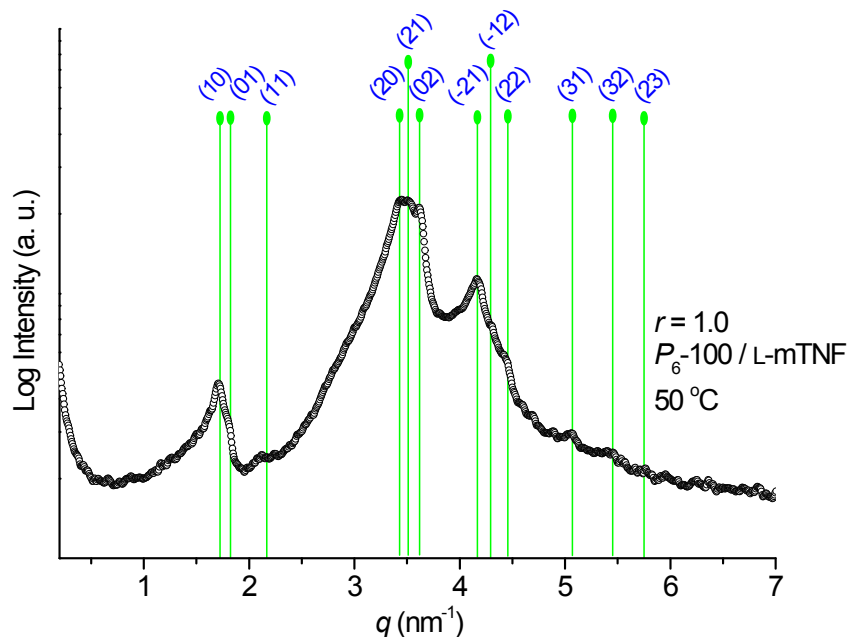


Figure S17. SAXS profile with proposed indexing of equimolar EDA complex of P_6 -100 doped with L-mTNF ($r = 1.0$) at 50 °C during the second heating process.

Table S5. SAXS/WAXS data for equimolar EDA complex of P_6 -100 doped with L-mTNF ($r = 1.0$) at 50 °C during the second heating process

| mesophase | hkl | d_{obs} [Å] | d_{calc} [Å] | lattice parameter [Å] | ρ_{calc}^a | |
|----------------------------------|-------|-------------------------|--------------------------|--------------------------|-------------------------|--|
| Col _{obs} -s (50 °C) | 100 | 36.7 | 36.7 | $a = 37.5$ | 1.07 g cm ⁻³ | |
| | 010 | 34.7 | 34.7 | $b = 35.5$ | | |
| $p2$ | 110 | 28.9 | 28.4 | $\gamma = 77.8^\circ$ | | |
| | 200 | 18.2 | 18.4 | | | |
| | 210 | 17.9 | 17.8 | | | |
| | 020 | 17.4 | 17.4 | | | |
| | -210 | 15.1 | 15.0 | | | |
| | -120 | 14.6 | 14.5 | | | |
| | 220 | 14.2 | 14.2 | | | |
| | 310 | 12.4 | 12.4 | | | |
| | 320 | 11.5 | 11.2 | | | |
| | 230 | 10.9 | 10.9 | | | |
| | | 4.4 (diffuse halo) | | | | |
| | | 001 | 3.32 | | | |

^a Density, ρ , was calculated as $\rho = M \cdot Z / (N_A \cdot V_{\text{unit cell}})$, where $V_{\text{unit cell}} = a \cdot b \cdot \sin \gamma \cdot c$, $Z = 4$ ($c = 3.32$ Å), and M is the average molecular weight of the repeat unit (899 g mol⁻¹) and doped L-mTNF (497 g mol⁻¹), which is calculated as $M = (899 + 497 \cdot r) / (1 + r) = 698$ g mol⁻¹.

3.2 SAXS/WAXS characterization and analysis for EDA complexes of P_9 -100 doped with L-mTNF

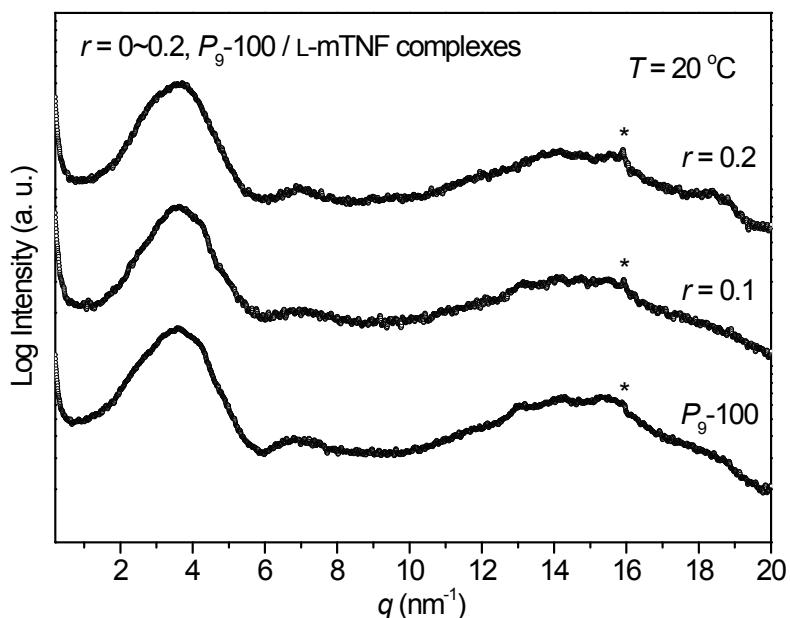


Figure S18. SAXS/WAXS patterns of undoped P_9 -100 and its EDA complexes doped with L-mTNF in the molar ratios $r = 0.1$ and 0.2 at $20\text{ }^\circ\text{C}$ during the second heating process, belonging to unidentified low order columnar phase (Col_x).

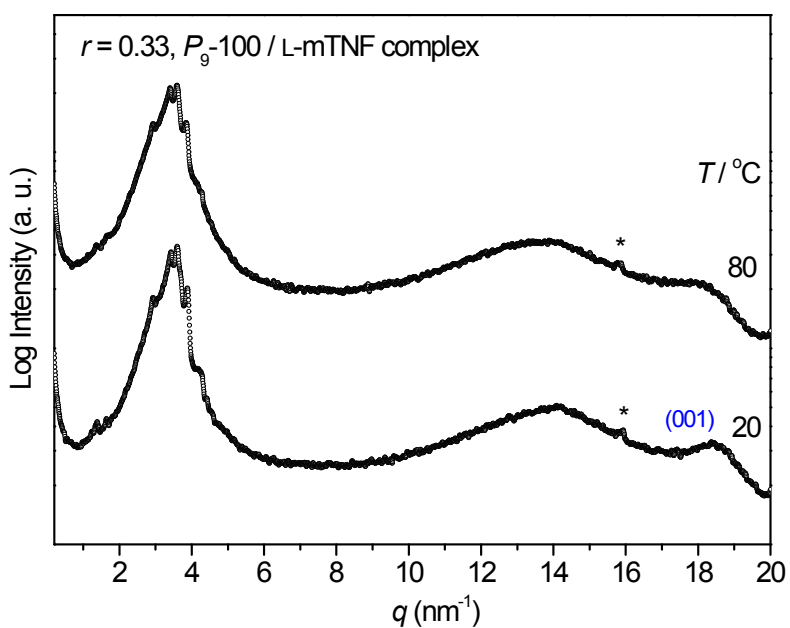


Figure S19. Variable-temperature SAXS/WAXS patterns of EDA complex of P_9 -100 doped with L-mTNF in the ratio $r = 0.33$ at indicated temperatures during the second heating process.

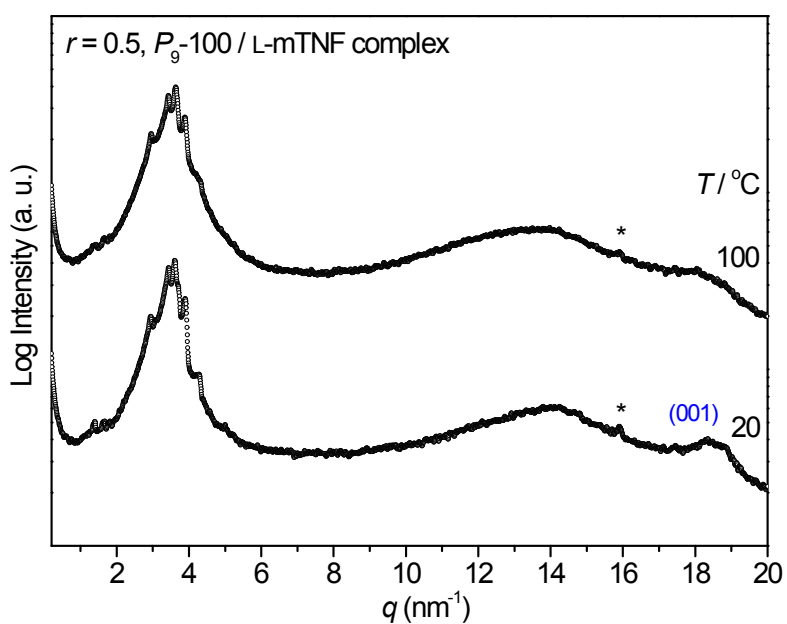


Figure S20. Variable-temperature SAXS/WAXS patterns of EDA complex of P_9 -100 doped with L-mTNF in the ratio $r = 0.5$ at indicated temperatures during the second heating process.

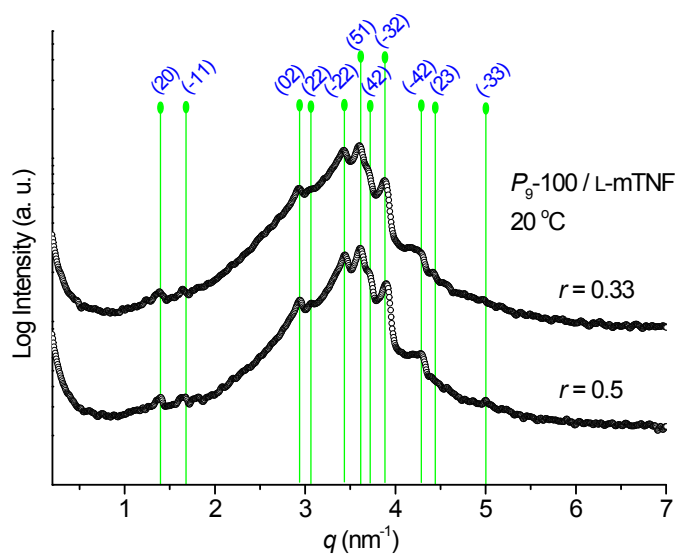


Figure S21. SAXS patterns with proposed indexing of EDA complex of P_9 -100 doped with L-mTNF in the molar ratios $r = 0.33$ and 0.5 at $20\text{ }^\circ\text{C}$ during the second heating process.

Table S6. SAXS/WAXS data for EDA complex of P_9 -100 doped with L-mTNF in the molar ratios $r = 0.33$ and 0.5 at $20\text{ }^\circ\text{C}$ during the second heating process

| mesophase | hkl | d_{obs} [Å] | d_{cacl} [Å] | lattice parameter [Å] | ρ_{calc}^a |
|--|-------|-------------------------|--------------------------|--------------------------|---|
| Col _{ob-s} (20 °C) $p2$ | 200 | 44.9 | 44.9 | $a = 90.6$ | 1.20 g cm ⁻³ ($r = 0.5$) |
| | -110 | 37.0 | 36.8 | $b = 43.2$ | |
| | 020 | 21.4 | 21.4 | $\gamma = 82.4^\circ$ | 1.24 g cm ⁻³ ($r = 0.33$) |
| | 220 | 20.5 | 20.4 | | |
| | -220 | 18.4 | 18.5 | | |
| | 510 | 17.4 | 17.4 | | |
| | 420 | 17.0 | 16.6 | | |
| | -320 | 16.2 | 16.4 | | |
| | -420 | 14.6 | 14.6 | | |
| | 230 | 14.2 | 14.2 | | |
| -330 | 12.5 | 12.3 | | | |
| | | 4.4 (diffuse halo) | | | |
| | | 3.39 ($r = 0.5$), | | | |
| 001 | | 3.41 ($r = 0.33$) | | | |

^a Density, ρ , was calculated as $\rho = M \cdot Z / (N_A \cdot V_{\text{unit cell}})$, where $V_{\text{unit cell}} = a \cdot b \cdot \sin \gamma \cdot c$, $Z = 12$ (c is 3.39 \AA for $r = 0.5$ and 3.41 \AA for $r = 0.33$), and M is the average molecular weight of the repeat unit (941 g mol^{-1}) and doped L-mTNF (497 g mol^{-1}), which is calculated as $M = (941 + 497 \cdot r) / (1 + r) = 793\text{ g mol}^{-1}$ (for $r = 0.5$) or 830 g mol^{-1} (for $r = 0.33$).

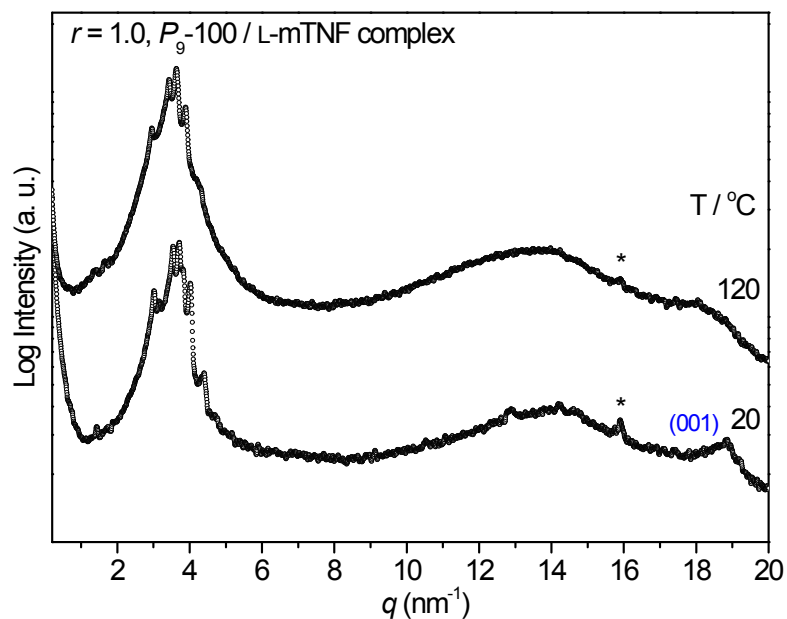


Figure S22. Variable-temperature SAXS/WAXS patterns of equimolar EDA complex of P_9 -100 doped with L-mTNF ($r = 1.0$) at indicated temperatures during the second heating process.

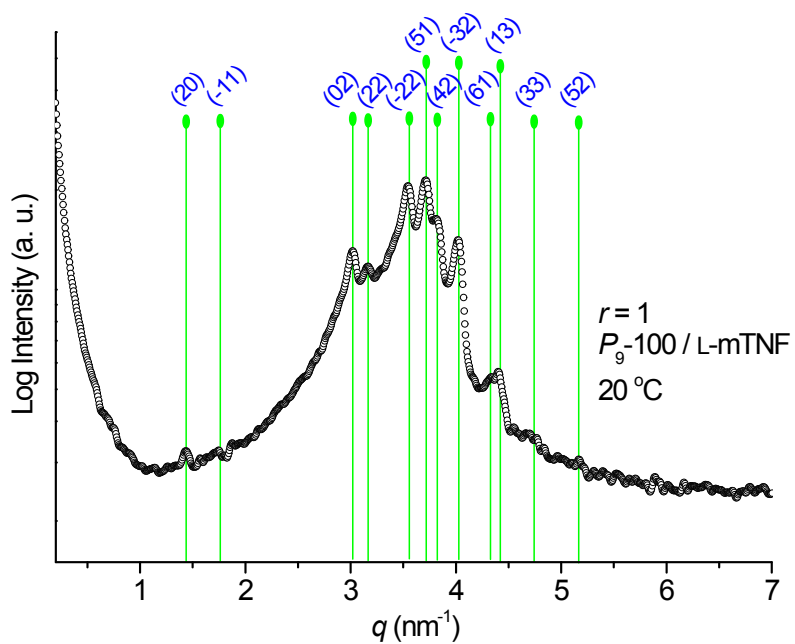


Figure S23. SAXS profile with proposed indexing of equimolar EDA complex of P_9 -100 doped with L-mTNF ($r = 1.0$) at 20 °C during the second heating process.

Table S7. SAXS/WAXS data for equimolar EDA complex of P_9 -100/L-mTNF ($r = 1.0$) at 20 °C during the second heating process

| mesophase | hkl | d_{obs} [Å] | d_{cacl} [Å] | lattice parameter [Å] | ρ_{calc}^a | |
|--|-------|-------------------------|--------------------------|--------------------------|-------------------------|--|
| Col _{ob-s} (20 °C) $p2$ | 200 | 43.6 | 44.9 | $a = 88.6$ | 1.17 g cm ⁻³ | |
| | -110 | 35.2 | 35.2 | $b = 42.3$ | | |
| | 020 | 20.8 | 20.8 | $\gamma = 79.8^\circ$ | | |
| | 220 | 20.0 | 20.2 | | | |
| | -220 | 17.6 | 17.6 | | | |
| | 510 | 17.0 | 17.2 | | | |
| | 420 | 16.4 | 16.5 | | | |
| | -320 | 15.6 | 15.7 | | | |
| | 610 | 14.5 | 14.5 | | | |
| | 130 | 14.2 | 14.1 | | | |
| | 330 | 13.3 | 13.5 | | | |
| | 520 | 12.2 | 12.3 | | | |
| | | 4.5 (diffuse halo) | | | | |
| | | 001 | 3.33 | | | |

^a Density, ρ , was calculated as $\rho = M \cdot Z / (N_A \cdot V_{\text{unit cell}})$, where $V_{\text{unit cell}} = a \cdot b \cdot \sin \gamma \cdot c$, $Z = 12$ ($c = 3.33$ Å), and M is the average molecular weight of the repeat unit (941 g mol⁻¹) and doped L-mTNF (497 g mol⁻¹), which is calculated as $M = (941 + 497 \cdot r) / (1 + r) = 719$ g mol⁻¹.

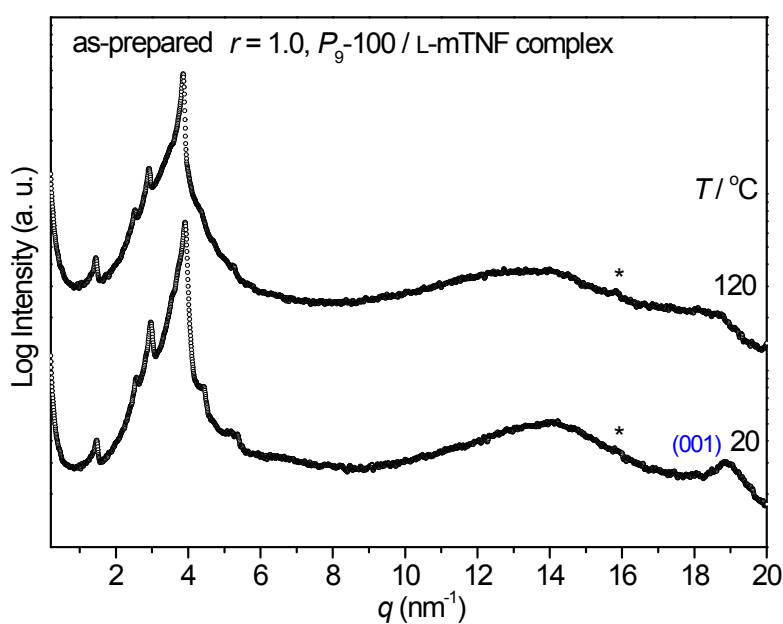


Figure S24. Variable-temperature SAXS/WAXS patterns of as-prepared equimolar EDA complex of P_9 -100 doped with L-mTNF ($r = 1.0$) at indicated temperatures during heating process.

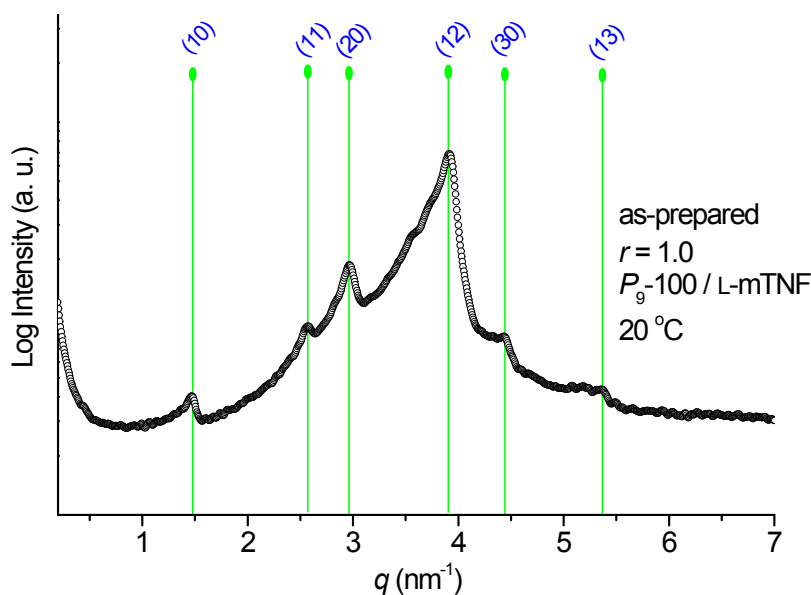


Figure S25. SAXS profile with proposed indexing of as-prepared equimolar EDA complex of P_9 -100 doped with L-mTNF ($r = 1.0$) at 20 °C during heating process.

Table S8. SAXS/WAXS data for as-prepared equimolar EDA complex of P_9 -100/L-mTNF ($r = 1.0$) at 20 °C during heating process

| mesophase | hkl | d_{obs} [Å] | d_{calc} [Å] | lattice parameter [Å] | ρ_{calc}^a |
|--|--------------------|-------------------------|--------------------------|--------------------------|-------------------------|
| $\text{Col}_{\text{h-s}}$ (20 °C) $p6mm$ | 100 | 42.7 | 42.7 | $a = 49.3$ | 1.03 g cm ⁻³ |
| | 110 | 24.5 | 24.5 | | |
| | 200 | 21.2 | 21.3 | | |
| | 120 | 16.0 | 16.0 | | |
| | 300 | 14.1 | 14.1 | | |
| | 130 | 11.7 | 11.8 | | |
| | 4.5 (diffuse halo) | | | | |
| | 001 | 3.32 | | | |

^a Density, ρ , was calculated as $\rho = M \cdot Z / (N_A \cdot V_{\text{unit cell}})$, where $V_{\text{unit cell}} = a^2 \cdot c \cdot \sqrt{3}/2$, $Z = 6$ ($c = 3.32$ Å), and M is the average molecular weight of the repeat unit (941 g mol⁻¹) and doped L-mTNF (497 g mol⁻¹), which is calculated as $M = (941 + 497 \cdot r) / (1 + r) = 719$ g mol⁻¹.

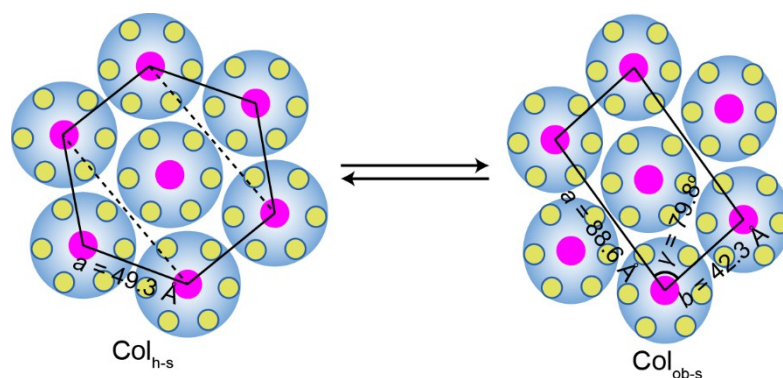


Figure S26. Schematic illustration of superstructure transformation between hexagonal columnar superlattice ($\text{Col}_{\text{h-s}}$) and oblique columnar superlattice ($\text{Col}_{\text{ob-s}}$) of equimolar EDA complex of P_9 -100/L-mTNF ($r = 1.0$).

The as-prepared equimolar EDA complex of P_9 -100/L-mTNF ($r = 1.0$) exhibited hexagonal columnar superlattice $\text{Col}_{\text{h-s}}$ ($p6mm$) of lattice parameter $a = 49.3 \text{ \AA}$ based on six-column bundles (Figure S24, S25 and Table S8). As shown in Figure S25, the SAXS pattern revealed that (12) peak was the strongest diffraction, which implied a strong electron density modulation with a period $\sqrt{7}$ times shorter than the (10) spacing; thus the coexistence of a hexagonal columnar lattice originating from co-stacking of side-chain TP discogens and acceptor L-mTNF with the confined polymer backbone probably in some stretched helical conformation, which as a whole constituting superlattice points well accounted for the hierarchical complex structure (Figure S26), resembling the assembled structure of neat P_9 -50 after a stepwise cooling process.² However, this polymeric equimolar EDA complex transformed into an oblique columnar superlattice $\text{Col}_{\text{ob-s}}$ ($p2$) with lattice parameter $a = 88.6$, $b = 42.3$ and $\gamma = 79.8^\circ$ after experiencing a melting process (Figure S22, S23 and Table S7). Such a superstructure transformation as schematically illustrated in Figure S26 from a symmetrical $\text{Col}_{\text{h-s}}$ to distorted $\text{Col}_{\text{ob-s}}$ accompanied with slightly increased theoretical density, further confirming the six-column bundles based oblique columnar superlattice.

3.3. SAXS/WAXS characterization and analysis for EDA complexes of monomers P_m -1 doped with L-mTNF

Table S9. SAXS/WAXS data for EDA complex of monomer P_6 -1 doped with L-mTNF in the molar ratio $r = 0.5$ at 50 °C

| mesophase | hkl | d_{obs} [Å] | d_{cacl} [Å] | lattice parameter [Å] | ρ_{calc}^a |
|-----------------------------|--------|-------------------------|--------------------------|--------------------------|-------------------------|
| Col _h (50 °C) | 100 | 17.5 | 17.5 | $a = 20.2$ | 1.06 g cm ⁻³ |
| | 110 | 10.1 | 10.1 | | |
| | $p6mm$ | 4.5 (diffuse halo) | | | |
| | 001 | 3.39 | | | |

^a Density, ρ , was calculated as $\rho = M \cdot Z / (N_A \cdot V_{\text{unit cell}})$, where $V_{\text{unit cell}} = a^2 \cdot c \cdot \sqrt{3}/2$, $Z = 1$ ($c = 3.39$ Å), and M is the average molecular weight of the repeat unit (899 g mol⁻¹) and doped L-mTNF (497 g mol⁻¹), which is calculated as $M = (899 + 497 \cdot r) / (1 + r) = 765$ g mol⁻¹.

Table S10. SAXS/WAXS data for equimolar EDA complex of monomer P_9 -1 doped with L-mTNF ($r = 1.0$) at 50 °C

| mesophase | hkl | d_{obs} [Å] | d_{cacl} [Å] | lattice parameter [Å] | ρ_{calc}^a |
|-----------------------------|--------|-------------------------|--------------------------|--------------------------|-------------------------|
| Col _h (50 °C) | 100 | 16.9 | 16.9 | $a = 19.5$ | 1.08 g cm ⁻³ |
| | 110 | 9.8 | 9.8 | | |
| | $p6mm$ | 4.4 (diffuse halo) | | | |
| | 001 | 3.35 | | | |

^a Density, ρ , was calculated as $\rho = M \cdot Z / (N_A \cdot V_{\text{unit cell}})$, where $V_{\text{unit cell}} = a^2 \cdot c \cdot \sqrt{3}/2$, $Z = 1$ ($c = 3.35$ Å), and M is the average molecular weight of the repeat unit (941 g mol⁻¹) and doped L-mTNF (497 g mol⁻¹), which is calculated as $M = (941 + 497 \cdot r) / (1 + r) = 719$ g mol⁻¹.

4. CD and UV-vis spectroscopic measurements of EDA complexes in solution and in solid-state film

For the preparation of film samples for CD and UV-vis spectroscopic measurements, the solutions of undoped TP-based side-chain discotic LCPs and their EDA complexes doped with variant ratios of chiral acceptor mTNF in chloroform (2 wt.%) were spin-coated on quartz plate substrates at 3000 rpm for 60 s.

The CD spectra measurements of the solid-state films on quartz plate substrate were examined at different rotation angles (Figure S27), which showed no significant difference, thus the possible linear dichroism (LD) can be precluded.³⁻⁵ The spectroscopic characteristics of as-prepared films by spin-coating manifested that discotic columns exhibited no dominant orientation or preferred alignment and thus presented macroscopic isotropy and mirror-image CD spectra induced by chiral enantiomeric acceptor dopants.

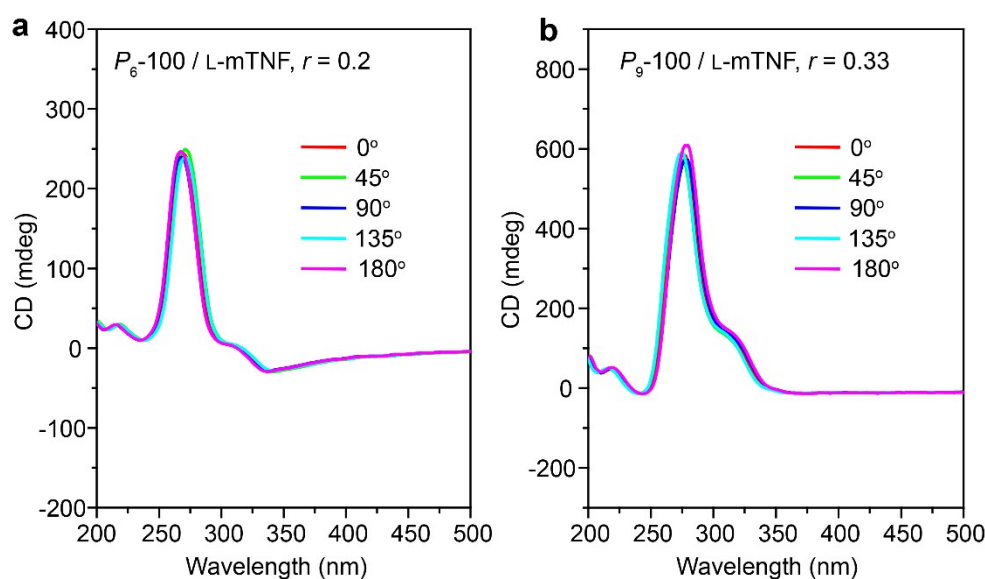


Figure S27. CD spectra of spin-coated solid state films of (a) $P_6-100/L-mTNF$ ($r = 0.2$) and (b) $P_9-100/L-mTNF$ ($r = 0.33$) measured at different rotation angles as indicated.

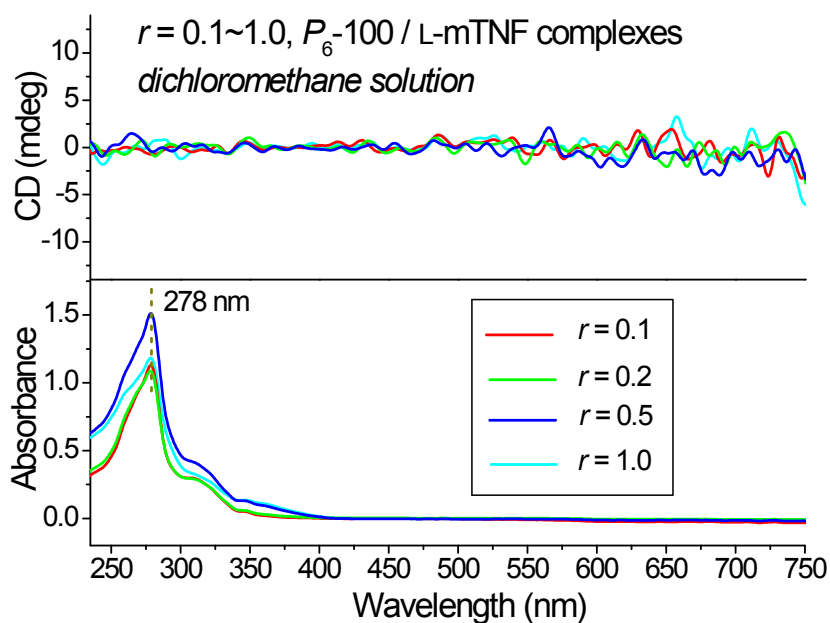


Figure S28. CD and UV-vis spectra of EDA complexes of P_6 -100 doped with L-mTNF at variant ratios in dichloromethane solution at concentration about 20 mg L^{-1} .

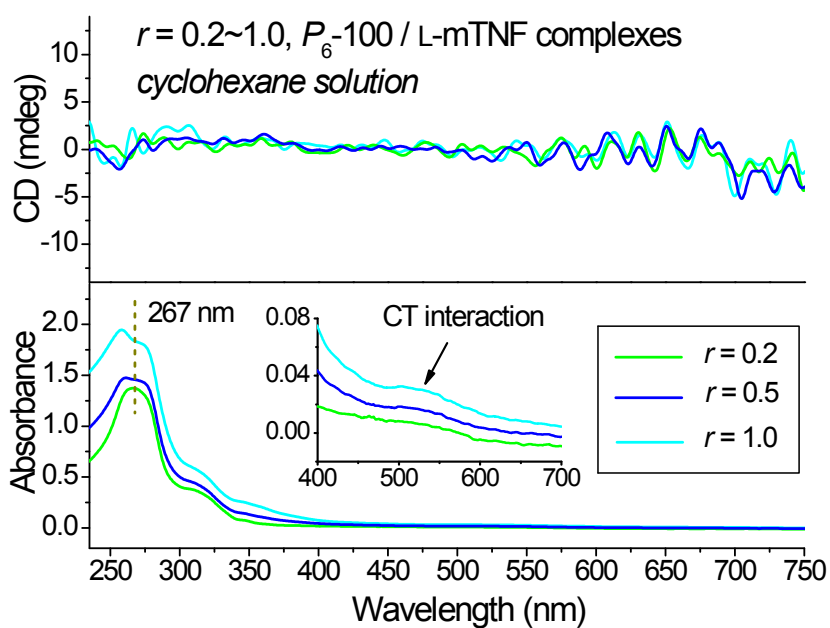


Figure S29. CD and UV-vis spectra of EDA complexes of P_6 -100 doped with L-mTNF at variant ratios in cyclohexane solution at concentration about 20 mg L^{-1} .

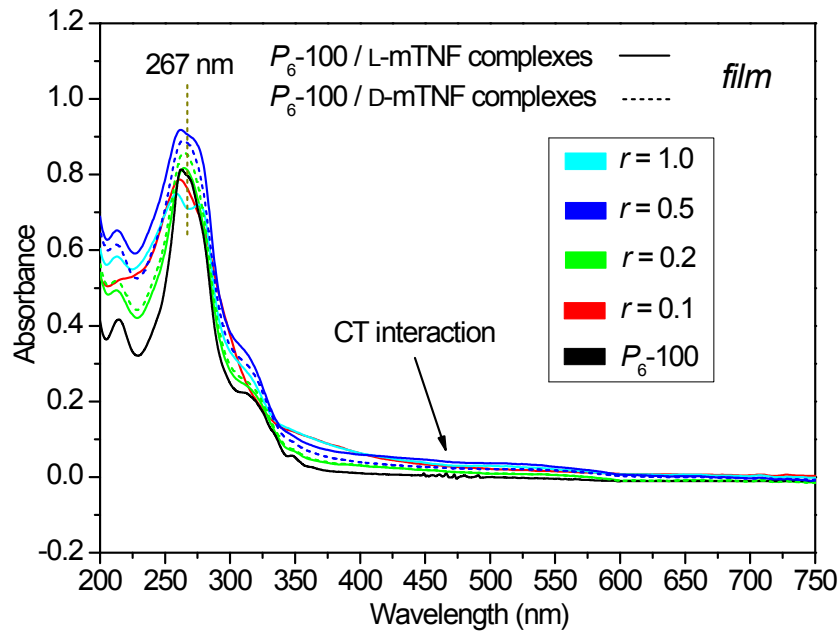


Figure S30. UV-vis spectra of EDA complexes of P_6 -100 doped with L-mTNF or D-mTNF at variant ratios in spin-coated solid-state film.

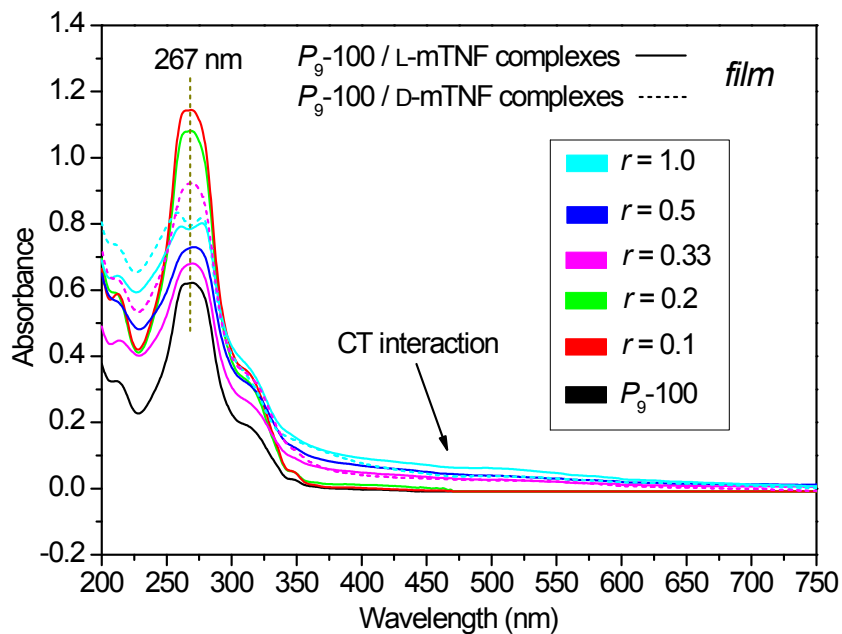


Figure S31. UV-vis spectra of EDA complexes of P_9 -100 doped with L-mTNF or D-mTNF in spin-coated solid-state film.

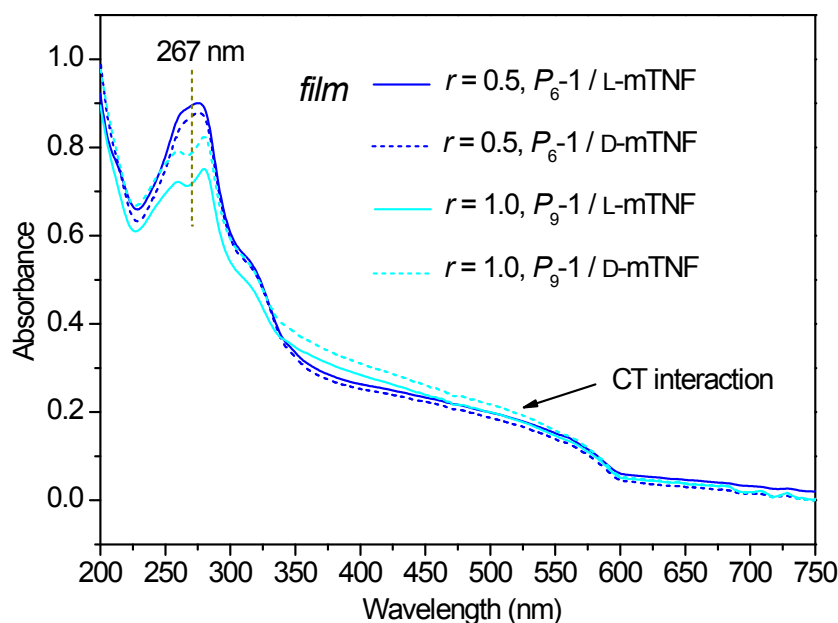


Figure S32. UV-vis spectra of EDA complexes of monomers P_6-1 or P_9-1 doped with L-mTNF or D-mTNF at ratios 0.5 or 1.0 in spin-coated solid-state film.

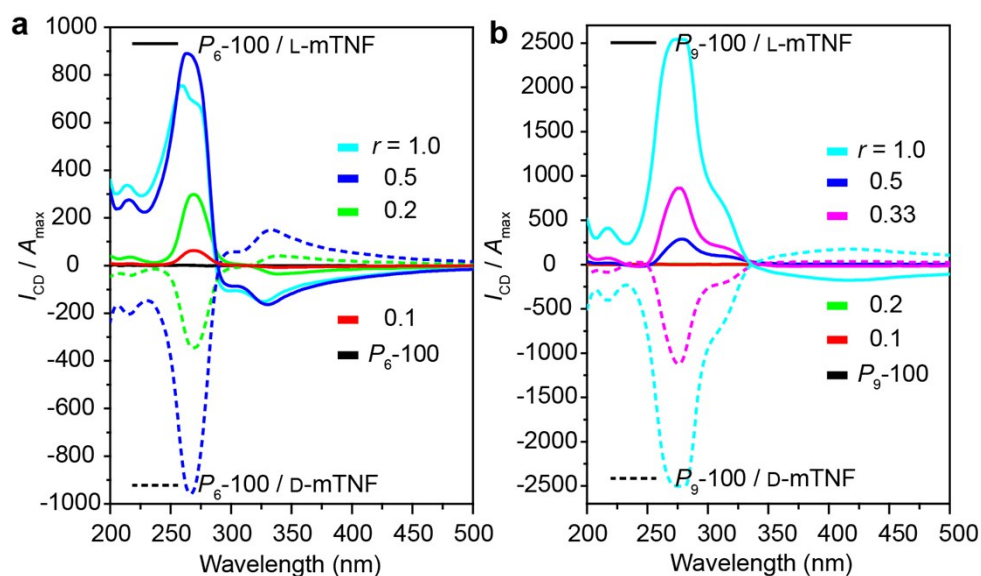


Figure S33. Comparative spectra of polymeric EDA complexes in solid-state films of (a) P_6-100 /D-mTNF or P_6-100 /L-mTNF and (b) P_9-100 /D-mTNF or P_9-100 /L-mTNF with varying molar ratio r of mTNF to TP unit, by comparing the intensity ratio of CD and UV-vis with $I_{CD}/I_{UV,max}$ as Y -axis to eliminate the influence of film thickness differences as suggested by Green and coworkers,⁶ where I_{CD} indicating measured CD intensity, and $I_{UV,max}$ approximately adopting the maximum absorbance at around 267 nm of UV spectra.

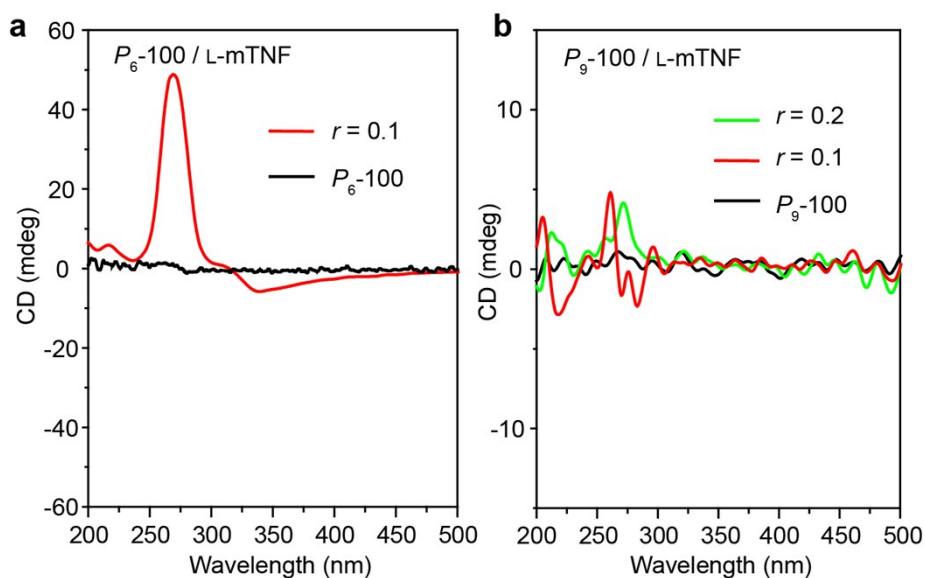


Figure S34. Enlarged CD spectra of polymeric EDA complexes in solid-state films of (a) P_6 -100/L-mTNF and (b) P_9 -100/L-mTNF with small ratio r values lower than the critical ratio, showing quite weak CD signals (Partial enlargement of Figure 4 in the main text for clarity).

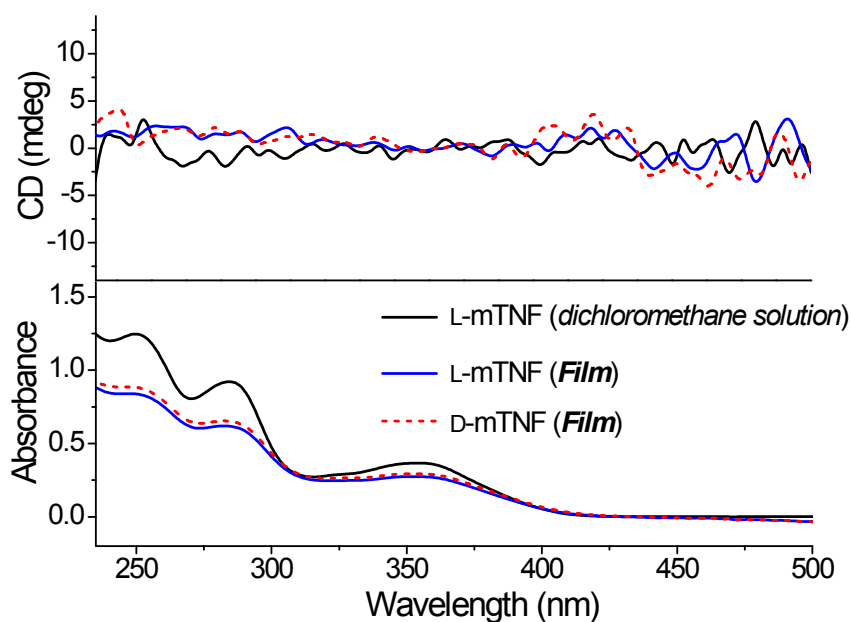


Figure S35. CD and UV-vis spectra of neat acceptor molecules L-mTNF or D-mTNF themselves in dichloromethane solution at concentration about 20 mg L^{-1} or in spin-coated solid state film.

5. Supplementary references

- 1 B. Mu, B. Wu, S. Pan, J. L. Fang and D. Z. Chen, *Macromolecules*, 2015, **48**, 2388-2398.
- 2 B. Mu, S. Pan, H. F. Bian, B. Wu, J. L. Fang and D. Z. Chen, *Macromolecules*, 2015, **48**, 6768-6780.
- 3 V. Percec, M. R. Imam, M. Peterca, D. A. Wilson, R. Graf, H. W. Spiess, V. S. K. Balagurusamy and P. A. Heiney, *J. Am. Chem. Soc.*, 2009, **131**, 7662-7677.
- 4 M. Wolffs, S. J. George, Z. Tomovic, S. C. J. Meskers, A. P. H. J. Schenning and E. W. Meijer, *Angew. Chem. Int. Ed.*, 2007, **46**, 8203-8205.
- 5 R. Kuroda and T. Honma, *Chirality*, 2000, **12**, 269-277.
- 6 M. M. Green, H. Ringsdorf, J. Wagner and R. Wüstefeld, *Angew. Chem. Int. Ed.*, 1990, **29**, 1478-1481.